Tetrahedron Letters xxx (xxxx) xxx

Contents lists available at ScienceDirect

Tetrahedron Letters

journal homepage: www.elsevier.com/locate/tetlet

Rational design of the benzothiazole-based fluorescent scaffold for tunable emission

Yong Ren, Dong Fan, Huazhou Ying, Xin Li *

College of Pharmaceutical Sciences, Zhejiang University, Hangzhou 310058, China

ARTICLE INFO

Article history:
Received 28 January 2019
Revised 8 March 2019
Accepted 11 March 2019
Available online xxxx

Keywords:
Benzothiazole
Fluorescence
Quantum yield

ABSTRACT

The 2-(2-hydroxyphenyl)-benzothiazole (HBT) fluorophore has attracted considerable attention due to its excited-state intramolecular proton transfer (ESIPT) based emission and its large Stokes shift. However, this fluorophore possesses several disadvantages including low quantum yield and short emission in the blue range. In this study, by coupling HBT at the *ortho*-, *meta*-, and *para*-positions to the hydroxyl group with different heterocycles to extend the conjugation system, we have successfully obtained new fluorophores with tunable emissions both in solution and in the solid-state (409–652 nm). Notably, all of the derivatives demonstrated improved quantum yields compared with the parent HBT structure. Moreover, selected compounds have been shown to shine brightly in live cells, indicating promising potential for bioimaging.

© 2019 Elsevier Ltd. All rights reserved.

Introduction

Fluorescent probes have been widely used in the fields of biological and environmental analysis due to their good photophysical properties, high sensitivity, good selectivity [1–12]. For the design of fluorescent probes, the choice of a proper fluorophore is of primary importance. Many fluorophores have been widely used for probe construction, such as BODIPY [4,13,14], coumarin, xanthene [15–17], cyanine [18–20], HBT [21–24]. Among them, HBT has attracted considerable attention because of the easy manipulation of its brightness due to its excited-state intramolecular proton transfer (ESIPT)-based emission [25–27]. HBT has been used in fluorescent molecular probes [7,8,23,28], molecular logic gates [7], fluorescent bioimaging [29–32], and for fundamental photophysical studies [33,34]. However, there are still some disadvantages that limit its application, such as low quantum yield and short emission wavelength. Generally, the emission wavelength of this fluorophore is in the range of 400–550 nm, which overlaps with the autofluorescence from biomolecules. To decrease the background signal from autofluorescence when bioimaging experiments are performed, it is preferable for the probe to emit in the green, red, or ideally, in the near infrared region.

It is well known that extending the π system of a fluorophore will red shift its emission, as illustrated by the gradual increase of the emission wavelength of the cyanine series of fluorophores [35]. However, the introduction of polyenes usually increases the lipophilicity of the fluorophore, decreasing their water solubility. In 2016, You and co-workers reported that the introduction of five-membered heterocyclic rings may also red shift the emission of fluorophores [36]. Inspired by this strategy, we have developed a series of HBT derivatives by introducing various substituted heterocycles to the HBT skeleton. The photophysical properties of the compounds were measured and the structure-photophysical property relationships are discussed. Notably, tunable emission was observed and all compounds show improved quantum yields compared with HBT. We have also confirmed the compatibility of the compounds with live cells and their brightness for live cell imaging.

Result and discussion

In solution HBT may emit *via* its phenolate form (blue emission) or an ESIPT-based mechanism (green emission, Fig. 1a). To red shift its emission, our strategy was to extend the conjugation system with its structure. Various five-membered heterocycles such as thiophene, furan and their derivatives were therefore introduced to the HBT skeleton (Fig. 1b), and the effect of the substitution position on the emission wavelength was determined.

The target fluorophores were synthesized as shown in Scheme 1. First, the starting compound **1** was synthesized according to a reported literature procedures [37]. Next, coupling **1** with bis(pinacolato)diboron in the presence of $PdCl_2$(dppf) and potassium acetate in 1,4-dioxane afforded the key intermediate **2**. Suzuki coupling

* Corresponding author.
E-mail address: lixin81@zju.edu.cn (X. Li).

https://doi.org/10.1016/j.tetlet.2019.03.029
0040-4039/© 2019 Elsevier Ltd. All rights reserved.

Please cite this article as: Y. Ren, D. Fan, H. Ying et al., Rational design of the benzothiazole-based fluorescent scaffold for tunable emission, Tetrahedron Letters, https://doi.org/10.1016/j.tetlet.2019.03.029

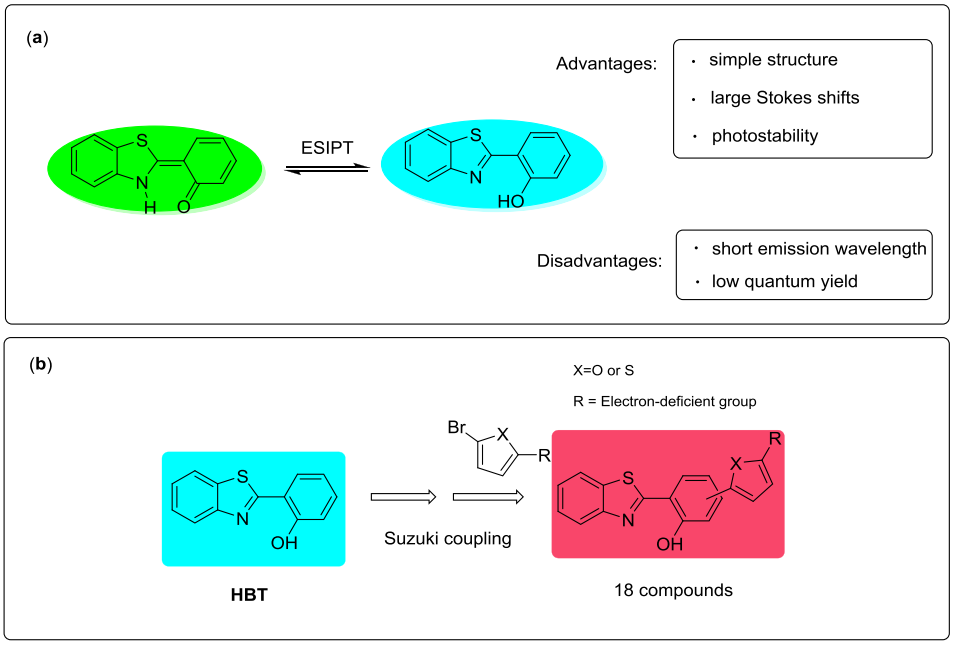

Fig. 1. ESIPT-based emission of HBT (a) and design rationale (b) of the HBT derivatives.

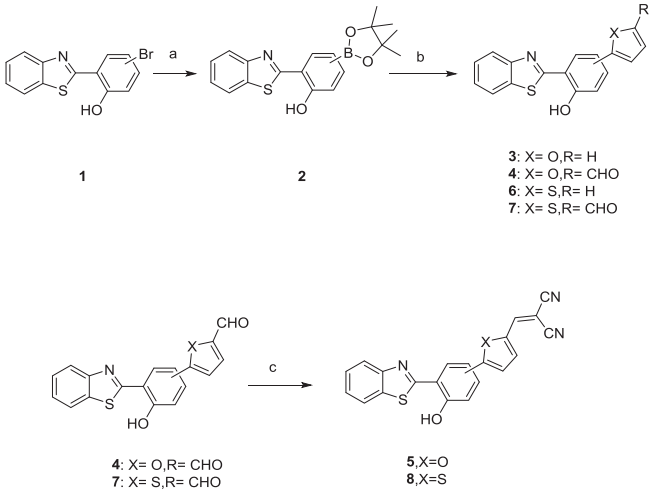

Scheme 1. Reagents and conditions: (a) bis(pinacolato)diboron (1 eq.), $PdCl_2$(dppf) (0.03 eq.), AcOK (3.5 eq.), 1,4-dioxane, reflux, overnight, 77%; (b) $Pd(OAc)_2$ (0.05 eq.), PPh_3 (0.2 eq.), K_2CO_3 (3.0 eq.), PhMe, reflux, overnight, 48–94%; (c) pyridine (0.06 eq.), malononitrile (3.0 eq.), EtOH, reflux, overnight, 23–72%.

reaction of **2** with 2-bromofuran, 2-bromothiophene or their analogues in the presence of $Pd(OAc)_2$, PPh_3 and potassium carbonate in anhydrous toluene gave the target compounds **3**, **4**, **6** and **7**. Further derivatization of compounds **4** and **7** with malononitrile employing the Knoevenagel condensation reaction gave compounds **5** and **8**, respectively. The structures of the final fluorophores were characterized by ^{1}H NMR, ^{13}C NMR spectroscopy and LCMS. Detailed synthetic data are given in the Supporting information.

With the HBT derivatives in hand (Scheme 2), their photophysical properties including absorption, emission, and quantum yields were measured in various solutions. Interestingly, these compounds demonstrate a wide range of emission (λ_{em}: 409–637 nm in CH_3CN; 491–612 nm in toluene) with large Stokes shifts (up to 230 nm in toluene; 232 nm in CH_3CN). Blue to red color emission was observed when the solutions were placed under a UV light (360 nm, 4 W) (Figs. 2 and S1). The emission wavelength was dependent on both the length of the conjugated system, and the position of the derivatization. To make clear the structure-photophysical property relationships, all data are shown in Tables 1, 2 and S1.

As shown by the data in Tables 1 and 2, extending the conjugated system works well to red shift its emission. Comparing with **HBT**, incorporation of either the furanyl (**3**) or thienyl (**6**) moiety significantly red-shifts the emission wavelengths by approximately 40–140 nm. Further extension of the conjugated system with a dicyanovinyl moiety (**5**, **8**) causes a more dramatic red-shifting effect with a further 50–100 nm shift (Tables 1, 2 and S1). Taking the data collected in acetonitrile for example, **HBT** exhibits an emission maximum at 369 nm, while its furanyl counterparts (**3-o**) show much longer emission maxima at 575 nm in acetonitrile. Notably, emission in the near-infrared region was observed for compound **5-p** and **8-p** (Fig. 3a). To further understand the relationship between the fluorescence properties and the chemical structure of these compounds, density functional theory (DFT) and time dependent density functional theory (TDDFT) calculations were carried out with the B3LYP/6-31+G(d) method basis set using the Gaussian 09 C.01 program. The optimized geometry, the highest occupied molecular orbital (HOMO) and the lowest unoccupied molecular orbital (LUMO) of selected compounds are presented in Figs. 4 and S2,S3. The HOMO–LUMO energy gap for **4-o** was determined as 4.223 eV which is reduced in **5-o** to 3.514 eV. The emission at a longer wavelength for **5-o** is well correlated with the reduced HOMO–LUMO energy gap.

After exploring the relationship between the substituent positions and emission wavelength, it was found that the incorporation of a furanyl/thienyl substituent in the *ortho*-position to the hydroxyl group induced the most dramatic red-shifting effect, followed by the *para*-position and then the *meta*-position (Fig. 3b). We hypothesize that extending the conjugated system of HBT makes it a more ICT (intramolecular charge transfer)-based fluorophore. The substitution of electron withdrawing furanyl/thienyl moiety in the *ortho*- or *para*-position is more favorable than the *meta*-position for the ICT effect, and therefore compounds with substituents in these two positions demonstrated the most dramatic red-shift effect [38].

Please cite this article as: Y. Ren, D. Fan, H. Ying et al., Rational design of the benzothiazole-based fluorescent scaffold for tunable emission, Tetrahedron Letters, https://doi.org/10.1016/j.tetlet.2019.03.029

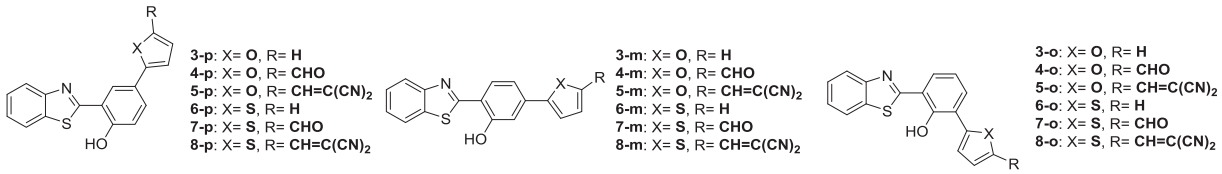

Scheme 2. Structures of the HBT derivatives.

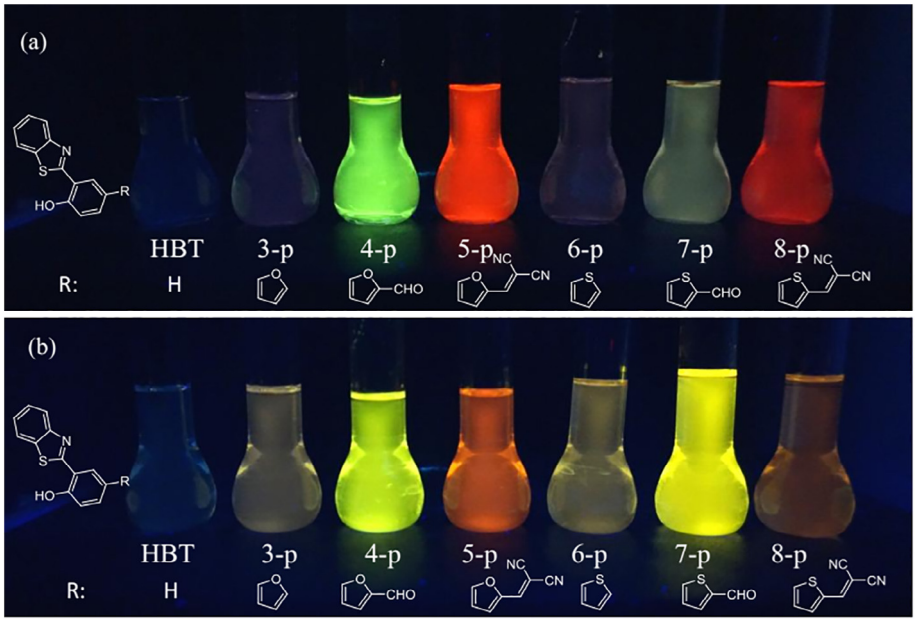

Fig. 2. (a) Fluorescence of selected compounds in CH_3CN (excited at 365 nm under a UV lamp). (b) Fluorescence of selected compounds in toluene (excited at 365 nm under a UV lamp).

Table 1
Optical properties of compounds **3-p**-**HBT** in CH_3CN.

Comp.	λ_{abs} (nm)	λ_{em} (nm)	Stokes shift (nm)	ε (M^{-1} cm^{-1})	Φ_F	Φ_F/Φ_{HBT}
3-p	363	553	190	3910	0.0140	9.96842631
4-p	336	553	217	3530	0.0103	7.3191883
5-p	426	623	197	4620	0.0333	23.742704
6-p	352	409	57	4230	0.0088	6.31737005
7-p	363	556	193	3900	0.0149	10.6180883
8-p	419	637	218	2980	0.0305	21.7810802
3-m	357	516	159	2540	0.0223	15.9247416
4-m	368	528	160	2840	0.0780	55.6561272
5-m	419	524	105	3500	0.0070	4.97869776
6-m	360	514	154	3500	0.0267	19.0248591
7-m	375	541	166	2680	0.0554	39.5317037
8-m	419	529	110	3520	0.0068	4.84030999
3-o	356	575	219	4040	0.0063	4.52995555
4-o	361	563	202	3680	0.0735	52.4665411
5-o	419	622	203	4130	0.1825	130.301992
6-o	354	586	232	1960	0.0119	8.52436485
7-o	365	566	201	3450	0.1334	95.2471313
8-o	414	618	204	3790	0.1471	105.01302
HBT	333	369	36	4220	0.0014	1

Furthermore, these compounds were also observed to demonstrate solvent-dependent emission properties. In general, the emission wavelength of the compounds tends to red shift as the polarity of the solvent increases. For instance, **5-o** shows an emission maxima at 603 nm (toluene)/605 nm (CH_2Cl_2)/622 nm (CH_3CN)/631 nm (EtOH)/635 nm (PBS), respectively (Fig. 3c). Other compounds showed similar patterns (Tables 1, 2 and S1). We hypothesize that this phenomenon should be due to the polar nature of the excited state which prefers a polar environment for stability. Consequently, a more polar solvent would decrease the energy gap between the HOMO and LUMO, and therefore red-shift its emission.

Interestingly, although all of the compounds showed low quantum yields in the region of 400–650 nm, their quantum yields were improved compared with the parent HBT in different organic solvents (Fig. 5). Interestingly, we found that the incorporation of

Please cite this article as: Y. Ren, D. Fan, H. Ying et al., Rational design of the benzothiazole-based fluorescent scaffold for tunable emission, Tetrahedron Letters, https://doi.org/10.1016/j.tetlet.2019.03.029

Table 2
Optical properties of compounds **3-p**-**HBT** in toluene.

Comp.	λ_{abs} (nm)	λ_{em} (nm)	Stokes shift (nm)	ε (M^{-1} cm^{-1})	Φ_F	Φ_F/Φ_{HBT}
3-p	370	550	180	3750	0.0228	2.21730818
4-p	339	553	214	3820	0.0803	7.81927843
5-p	436	600	164	4230	0.0230	2.24172205
6-p	365	555	190	4380	0.0151	1.46738319
7-p	350	562	212	4270	0.0910	8.86414898
8-p	426	606	180	4600	0.0152	1.4841833
3-m	363	520	157	5020	0.0707	6.88843995
4-m	374	532	158	3780	0.0778	7.5825541
5-m	425	496	71	4250	0.0151	1.47461093
6-m	366	518	152	3460	0.0849	8.27016456
7-m	380	535	155	4180	0.0696	6.77689507
8-m	425	491	66	4130	0.0148	1.44611956
3-o	364	581	217	2960	0.0195	1.89976061
4-o	364	568	204	3440	0.0874	8.50962898
5-o	425	603	178	4080	0.1342	13.0738351
6-o	359	589	230	3410	0.0210	2.05012388
7-o	371	578	207	3730	0.1528	14.887644
8-o	421	612	191	3900	0.1565	15.2478176
HBT	336	518	182	3470	0.0103	1

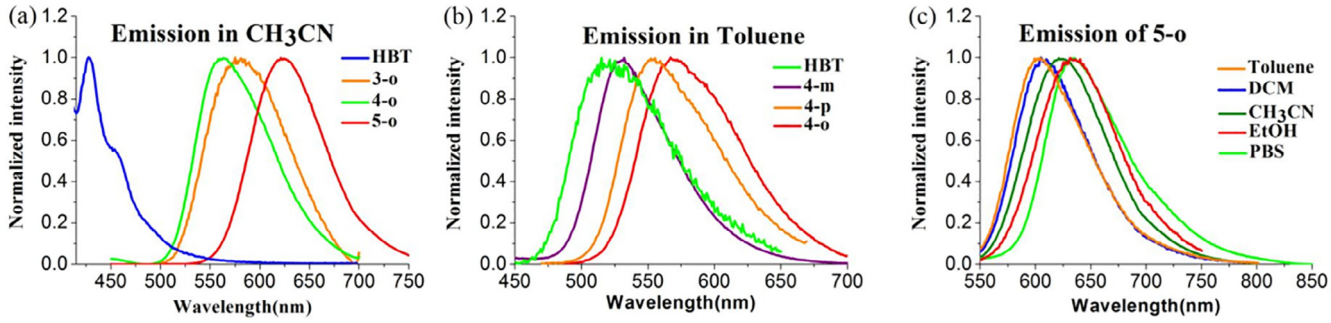

Fig. 3. (a) Fluorescence spectra of selected compounds in CH_3CN; (b) Fluorescence spectra of selected compounds in toluene; (c) Emission spectra of **5-o** in different solvents.

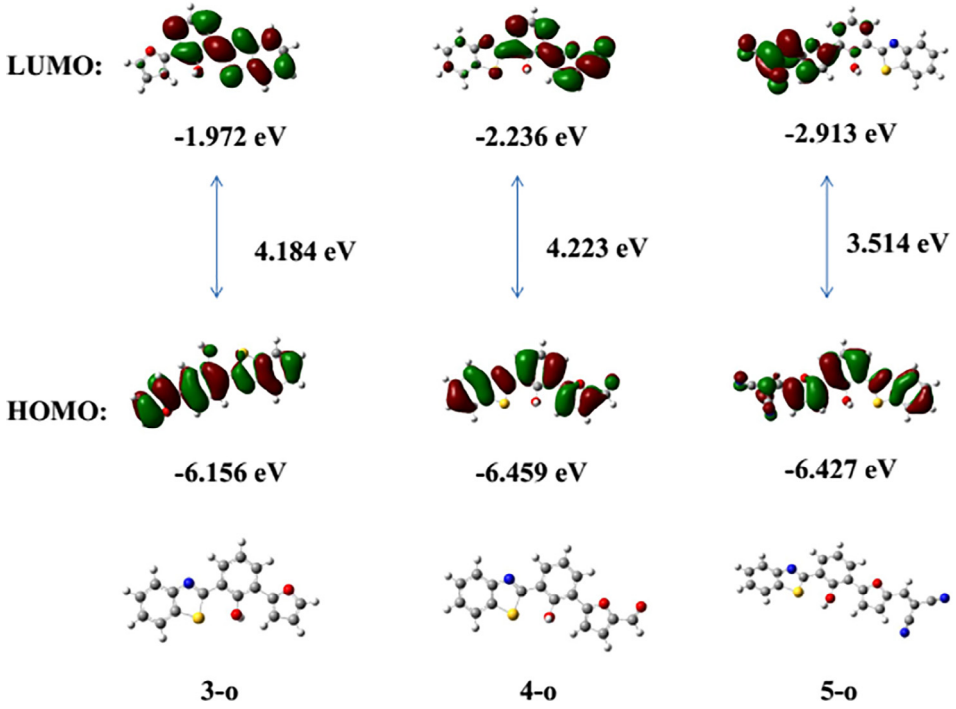

Fig. 4. Energy minimization structures of selected compounds and their HOMO-LUMO distribution.

Please cite this article as: Y. Ren, D. Fan, H. Ying et al., Rational design of the benzothiazole-based fluorescent scaffold for tunable emission, Tetrahedron Letters, https://doi.org/10.1016/j.tetlet.2019.03.029

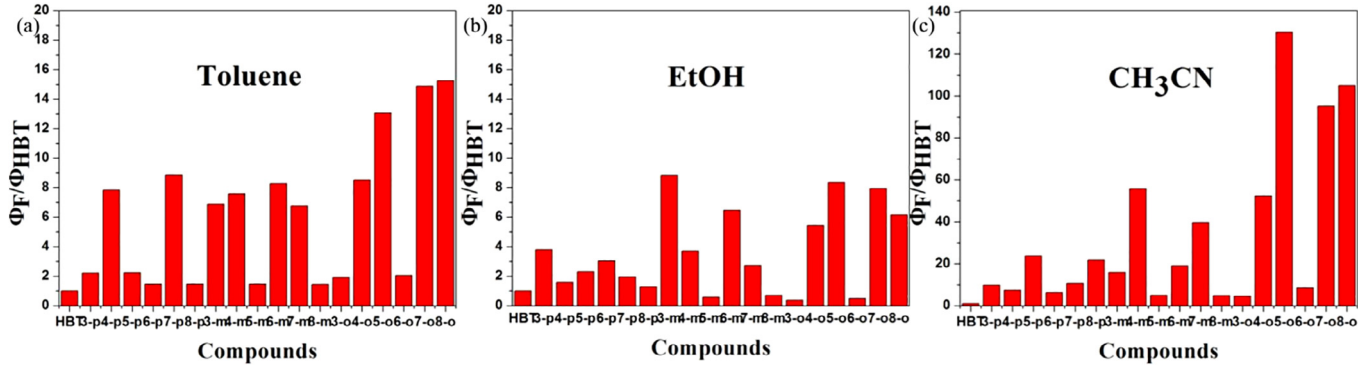

Fig. 5. All compounds show improved quantum yields compared with **HBT** in organic solvents (Y-axis: Φ_F/Φ_{HBT}, where Φ_F is the quantum yield of the newly synthesized compounds and Φ_{HBT} is that of HBT.

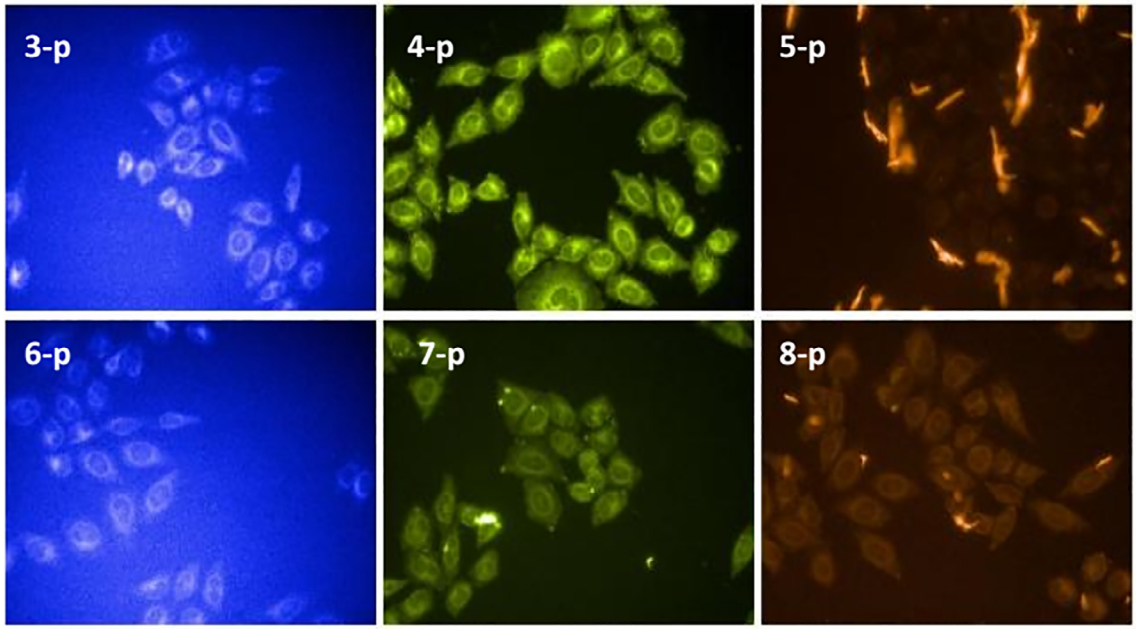

Fig. 6. Fluorescence microscopic image of HeLa cells dosed with compound **3-p**, **4-p**, **5-p**, **6-p**, **7-p**, **8-p** (10) μM for 30 min **3-p** and **6-p**: Ex: 360 nm-400 nm, Em: 410 nm-480 nm; **4-p** and **7-p**: Ex: 360 nm-400 nm, Em: 530 nm-590 nm; **5-p** and **8-p**: Ex: 410 nm-430 nm, Em: 580 nm-650 nm.

thiophene or furan at the *ortho*-position to the hydroxyl group usually resulted in higher quantum yields than those at the *meta*- or *para*-position. This may result from the fact that the introduction of thiophene or furan at the *ortho*-position restricts the twist of the molecule, reducing energy consumption. For instance, when furan was introduced, **5-o** shows much higher quantum yield ($\Phi_F = 0.1342$) than **5-m** ($\Phi_F = 0.0151$) and **5-p** ($\Phi_F = 0.0230$) in toluene (Table 2).

Finally, these compounds were observed to emit in the solid state (Fig. S4). Furthermore, the emission color of these compounds in the solid state is also significantly dependent on the length of the conjugated system, with red emission being observed for compounds bearing the longest conjugated system. Also, substitution at the *ortho*-position to the hydroxyl group resulted in the brightest emission. All these observations agree well with those obtained in solution. We argue that the solid-state fluorescence of the compounds is desirable as it will not cause aggregation-induced quenching.

To test the applicability of the compounds for live cell imaging experiments, representative compounds **3-p**, **4-p**, **5-p**, **6-p**, **7-p**, **8-p** were fed to HeLa cells. After an incubation time of 30 min, the cells were washed with PBS and then imaged under microscopy. As shown in Fig. 6, all of the tested compounds demonstrate good cell membrane permeability and shine brightly in live cells. Interestingly, their emission color agrees well with that observed in solutions and red-shifts with the conjugated system becoming longer. Notably, for selected compounds, for example **3-p**, **4-p** and **5-p**, their emission color separate well with each other, suggesting their potential for the multi-color imaging of live cells.

Conclusion

By coupling HBT with furanyl/thienyl rings, a series of novel compounds with tunable emission were obtained. All of the compounds demonstrate red-shift emissions with their conjugated system getting longer, and some compounds were observed to emit in the near-infrared region. It was determined that the position of derivatization significantly effects the photophysical properties of the compounds, and the *ortho*-position to the hydroxyl group is the ideal derivatization position for red-shifting emission. The feasibility of the compounds for live cell imaging was also confirmed and representative compounds were found to shine brightly in live

Please cite this article as: Y. Ren, D. Fan, H. Ying et al., Rational design of the benzothiazole-based fluorescent scaffold for tunable emission, Tetrahedron Letters, https://doi.org/10.1016/j.tetlet.2019.03.029

cells. Given the tunable emission of the compounds and their improved quantum yields compared with the parent HBT structure, we believe that they may work as alternatives for future fluorescent probe development.

Acknowledgments

We appreciate Prof. Jianzhong Chen for the instruction on DFT and TDDFT calculations, Dr Ying Dong for the generous help in cell imaging experiments, and Dr Jianyang Pan for collecting the NMR data. This work was supported by the National Natural Science Foundation of China (21778048, 21642007), and the Natural Science Foundation of Zhejiang province (LR18H300001).

Appendix A. Supplementary data

Supplementary data to this article can be found online at https://doi.org/10.1016/j.tetlet.2019.03.029.

References

[1] B.N.G. Giepmans, S.R. Adams, M.H. Ellisman, R.Y. Tsien, Science 312 (2006) 217.
[2] I.L. Medintz, H.T. Uyeda, E.R. Goldman, H. Mattoussi, Nat. Mater. 4 (2005) 435.
[3] S. Weiss, Science 283 (1999) 1676.
[4] N. Boens, V. Leen, W. Dehaen, Chem. Soc. Rev. 41 (2012) 1130.
[5] H.N. Kim, W.X. Ren, J.S. Kim, J. Yoon, Chem. Soc. Rev. 41 (2012) 3210.
[6] Y. Zhou, J.F. Zhang, J. Yoon, Chem. Rev. 114 (2014) 5511.
[7] J. Wu, W. Liu, J. Ge, H. Zhang, P. Wang, Chem. Soc. Rev. 40 (2011) 3483.
[8] J.F. Zhang, Y. Zhou, J. Yoon, J.S. Kim, Chem. Soc. Rev. 40 (2011) 3416.
[9] S. Luo, E. Zhang, Y. Su, T. Cheng, C. Shi, Biomaterials 32 (2011) 7127.
[10] H.M. Kim, B.R. Cho, Acc. Chem. Res. 42 (2009) 863.
[11] M. Vendrell, D.T. Zhai, J.C. Er, Y.T. Chang, Chem. Rev. 112 (2012) 4391.
[12] M.H. Lee, J.S. Kim, J.L. Sessler, Chem. Soc. Rev. 44 (2015) 4185.
[13] A. Loudet, K. Burgess, Chem. Rev. 107 (2007) 4891.
[14] G. Ulrich, R. Ziessel, A. Harriman, Angew. Chem. Int. Ed. 47 (2008) 1184.
[15] M. Sibrian-Vazquez, J.O. Escobedo, M. Lowry, F.R. Fronczek, R.M. Strongin, J. Am. Chem. Soc. 134 (2012) 10502.
[16] Y. Yang, M. Lowry, C.M. Schowalter, S.O. Fakayode, J.O. Escobedo, X. Xu, H. Zhang, T.J. Jensen, F.R. Fronczek, I.M. Warner, R.M. Strongin, J Am. Chem. Soc. 128 (2006) 14081.
[17] T. Miura, Y. Urano, K. Tanaka, T. Nagano, K. Ohkubo, S. Fukuzumi, J. Am. Chem. Soc. 125 (2003) 8666.
[18] W. Cao, E.M. Sletten, J. Am. Chem. Soc. 140 (2018) 2727.
[19] G.T. Dempsey, M. Bates, W.E. Kowtoniuk, D.R. Liu, R.Y. Tsien, X. Zhuang, J. Am. Chem. Soc. 131 (2009) 18192.
[20] H.-J. Chen, C.Y. Chew, E.-H. Chang, Y.-W. Tu, L.-Y. Wei, B.-H. Wu, C.-H. Chen, Y.-T. Yang, S.-C. Huang, J.-K. Chen, I.C. Chen, K.-T. Tan, J. Am. Chem. Soc. 140 (2018) 5224.
[21] M.A. Rios, M.C. Rios, J. Phys. Chem. 102 (1998) 1560.
[22] C. Rodriguez-Rodriguez, N.S. de Groot, A. Rimola, A. Alvarez-Larena, V. Lloveras, J. Vidal-Gancedo, S. Ventura, J. Vendrell, M. Sodupe, P. Gonzalez-Duarte, J. Am. Chem. Soc. 131 (2009) 1436.
[23] X.F. Yang, Q. Huang, Y.G. Zhong, Z. Li, H. Li, M. Lowry, J.O. Escobedo, R.M. Strongin, Chem. Sci. 5 (2014) 2177.
[24] T.I. Kim, H.J. Kang, G. Han, S.J. Chung, Y. Kim, Chem. Commun. (2009) 5895.
[25] P. Yang, J. Zhao, W. Wu, X. Yu, Y.T. Liu, J. Org. Chem. 77 (2012) 6166.
[26] S. Goswami, S. Das, K. Aich, B. Pakhira, S. Panja, S.K. Mukherjee, S. Sarkar, Org. Lett. 15 (2013) 5412.
[27] D. Maity, V. Kumar, T. Govindaraju, Org. Lett. 14 (2012) 6008.
[28] C.-C. Hsieh, C.-M. Jiang, P.-T. Chou, Acc. Chem. Res. 43 (2010) 1364.
[29] X. Li, R.-R. Tao, L.-J. Hong, J. Cheng, Q. Jiang, Y.-M. Lu, M.-H. Liao, W.-F. Ye, N.-N. Lu, F. Han, Y.-Z. Hu, Y.-H. Hu, J. Am. Chem. Soc. 137 (2015) 12296.
[30] K.C. Song, J.S. Kim, S.M. Park, K.-C. Chung, S. Ahn, S.-K. Chang, Org. Lett. 8 (2006) 3413.
[31] S.K. Patra, S.K. Sheet, B. Sen, K. Aguan, D.R. Roy, S. Khatua, J. Org. Chem. 82 (2017) 10234.
[32] Y. Zhang, L. Guan, H. Yu, Y. Yan, L. Du, Y. Liu, M. Sun, D. Huang, S. Wang, Anal. Chem. 88 (2016) 4426.
[33] G.-J. Zhao, K.-L. Han, Acc. Chem. Res. 45 (2012) 404.
[34] M.A. Ríos, M.C. Ríos, J. Phys. Chem. 102 (1998) 1560.
[35] W. Sun, S. Guo, C. Hu, J. Fan, X. Peng, Chem. Rev. 116 (2016) 7768.
[36] Y. Cheng, G. Li, Y. Liu, Y. Shi, G. Gao, D. Wu, J. Lan, J. You, J. Am. Chem. Soc. 138 (2016) 4730.
[37] S. Samanta, S. Das, P. Biswas, J. Org. Chem. 78 (2013) 11184.
[38] Z.R. Grabowski, K. Rotkiewicz, W. Rettig, Chem. Rev. 103 (2003) 3899.

Please cite this article as: Y. Ren, D. Fan, H. Ying et al., Rational design of the benzothiazole-based fluorescent scaffold for tunable emission, Tetrahedron Letters, https://doi.org/10.1016/j.tetlet.2019.03.029